Injury, Int. J. Care Injured 50 (2019) 1883–1888

Contents lists available at ScienceDirect

Injury

journal homepage: www.elsevier.com/locate/injury

Effect of fracture levels on the strength of bone-implant constructs in subtrochanteric fracture models fixed using short cephalomedullary nails: A finite element analysis

Chul-Young Jang[a,1], Sun-Hee Bang[b,1], Won-Hyeon Kim[c], Sung-Jae Lee[b], Hyung-Min Lee[a], Dae-Kyung Kwak[a], Je-Hyun Yoo[a,*]

[a] Department of Orthopaedic Surgery, Hallym University Sacred Heart Hospital, Hallym University College of Medicine, Anyang, Republic of Korea
[b] Department of Biomedical Engineering, Inje University, Gimhae, Republic of Korea
[c] Department of Mechanical Engineering, Sejong University, Seoul, Republic of Korea

ARTICLE INFO

Article history:
Accepted 10 August 2019

Keywords:
Subtrochanteric fracture
Short cephalomedullary nail
Finite element analysis
Failure

ABSTRACT

Objectives: This study was conducted to investigate the stress around nails and cortical bones in subtrochanteric (ST) fractures fixed using short cephalomedullary nails (CMNs) in finite element models (FEMs) and to determine the appropriate short CMN type for different fracture levels.
Methods: The following three types of short CMNs were used: type A, which is 170 mm in length and has 1 distal locking screw; type B, 200 mm in length and 1 distal screw; and type C, 200 mm in length and 2 distal screws. A total of 24 FEMs were tested on a transverse ST fracture at 8 levels [0, 10, 20, 25, 30, 35, 40 and 50 mm below the lower margin of lesser trochanter (LT)], and were fixed using 3 different CMN types. Finite element analysis was then performed to evaluate the stress around the cortical bones and the CMNs under the assumption of anatomical reduction and fracture gap of 1 mm.
Results: Peak von Mises stress (PVMS) was greatest on the cortical bone around the distal screw hole and was greater than the yield strength at fracture levels $\geq$ 35 mm below the LT in FEMs fixed with type A and B. In contrast, FEMs fixed with type C showed PVMS less than the yield strength at all fracture levels. The PVMS within the implant was greater than the yield strength at the junction of the nail with the distal screw and distal screw itself at fracture levels $\geq$ 35 mm below the LT in FEMs fixed using type A. Conversely, in FEMs fixed using type B and C, all PVMSs within the implant were less than the yield strength, regardless of the fracture level.
Conclusion: Short CMNs 170 or 200 mm in length with 1 distal screw may be used in a limited manner in high ST transverse fractures under the assumptions of anatomical reduction and fracture gap $\leq$ 1 mm. Meanwhile, short CMN 200 mm in length with 2 distal screws may be an available treatment option in most of ST transverse fractures regardless of the fracture level under the same set of assumptions.

Introduction

It is challenging to achieve anatomical reduction and stable fixation of subtrochanteric (ST) fracture by surgical means. Intense medial compression and lateral tensile forces are concentrated in the fracture region, and these deforming forces make reduction and fixation difficult. These obstacles and the low vascularity in the fracture region have challenged orthopedic surgeons with problems of malunion, nonunion, and implant failures [1].

Cephalomedullary nails (CMNs), due to their biomechanical superiority to extramedullary implants, have been used as the preferred devices for treating ST fractures [2,3]. Good clinical outcomes have recently been reported following treatment of ST fractures using CMNs [4–6]. Short and long CMNs are both currently used in the management of ST fractures. In theory, long CMNs have a biomechanical advantage over short CMNs [5]. They have a longer working length than short CMNs and are designed for improved stability while minimizing the diaphyseal stress risers associated with short CMNs [7]. Short CMNs are associated with shorter operation and fluoroscopy times, less blood loss, and lower

* Corresponding author at: Department of Orthopaedic Surgery, Hallym University Sacred Heart Hospital, Hallym University College of Medicine, 22 Gwanpyeong-ro 170beon-gil, Dongan-gu, Anyang-si, Gyeonggi-do, 14068, Republic of Korea.
E-mail address: oships@hallym.ac.kr (J.-H. Yoo).
[1] These authors contributed equally to this work and are the first authors of this work.

https://doi.org/10.1016/j.injury.2019.08.014
0020-1383/

cost than long CMNs [8,9]. The life expectancy and incidence of osteoporotic or atypical ST fractures in elderly patients are expected to increase in the future. Short operation time and decreased blood loss during hip fracture surgery in elderly patients can reduce blood transfusion rate, which is associated with long-term mortality [10]. The use of short CMNs would be more advantageous than the use of long CMNs, especially in elderly patients with ST fractures, when the associated shorter operation time and lesser blood loss are considered.

There is currently a paucity of high-quality evidences comparing short and long CMNs in the management of ST fractures [8]. Furthermore, the indications for short and long CMNs are unclear, and there is little information on the appropriate standard short CMN to be used at various levels of ST fracture. The validation of these issues, which are of concern to patients with ST fractures, is met with several problems.

The aim of this finite element analysis (FEA) was to investigate the stress around the CMNs and the cortical bones at various fracture levels using short CMNs of different lengths with varying numbers of distal locking screws and to determine the appropriate short CMN type indicated at different levels of ST fractures.

Materials and methods

Finite element model (FEM)

A three-dimensional (3D) femoral FEM, verified in a previous study was used in this study [11]. Computed tomography (CT)-scanned of a left intact femur was performed at 1.0 mm transverse resolution in 1.0 mm increments. The geometry of the femur and medullary canal surfaces were reconstructed using CT slice images in the Mimics (version 21.0, Materialise, Belgium) program. To reproduce ST fracture models, transverse fracture lines were produced at 8 levels in the ST region [0, 10, 20, 25, 30, 35, 40 and 50 mm below the lower margin of the lesser trochanter (LT)] on each femur model using ABAQUS (version 6.14, Dassault Systems, France).

Short Gamma 3 CMNs (Stryker, Mahwah, NJ, USA) were used in this study. They were divided into the following 3 types according to nail length and number of distal locking screws as follows: type A CMN, which is 170 mm in length with 1 distal locking screw; type B CMN, which is 200 mm in length with 1 distal locking screw; and type C CMN, which is 200 mm in length with 2 distal locking screws. Other features were identical for all short CMN types, unlike the nail length and the number of distal locking screws, which varied. These features include the 12.0-mm nail diameter, the 125°-caput-collum-diaphyseal angle, the 100-mm lag screw length, and the 40-mm distal locking screw length. The geometry of all nail configurations was constructed in the intramedullary canal of each fractured FEM using ABAQUS. The lag screw was inserted into the center-to-center of the femoral head, and the tip-apex distance was set to 22.92 mm in summation of the anterior-posterior and lateral views. Anatomical reduction and 1-mm fracture gap were assumed in all the models.

Eight-noded hexadral elements and 4-noded tetrahedral elements, created using the automatic solid and mesh generation program (ABAQUS), were used to build up the mesh of the fractured femur model and the Gamma 3 CMNs. These elements enabled the definition of the different material properties and maintained contact conditions in the fracture plane.

Material properties

In the FEM used in this study, it was assumed that the bone structure has homogeneous and isotropic linear properties. To assign cancellous bone property to the femoral model, the elastic modulus was calculated based on the referred averaged CT Hounce field unit (HU) value of 120.8 [12]. The following bone density-HU and elastic modulus-bone density relationships were used [13,14] :

$$\rho = 131000 + 1067\ \mathrm{HU}$$

$$\mathrm{E} = 6850\ \rho^{1.49}$$

where ρ is the apparent density (g/cm^3); and E is the elastic modulus (MPa). The material properties of the femoral cortical bone and nail were referenced from earlier publications (Table 1) [15,16]. Titanium alloy (TI6Al4V) was used for the Gamma 3 CMNs for the purpose of analysis. Different material properties were assigned to different femoral regions.

Boundary and loading condition

Assuming the 1-leg stance is taken during normal ambulation, a peak load of 2058 N, which is 300% of the body weight, was applied to the femoral head [17]. An additional 686 N, which is 100% of the body weight, was then applied considering the abductor muscle forces acting on the external side. The 2 forces were acting at an angle of 20° from the vertical line in the frontal plane (Fig. 1).

A "tie" contact condition was applied in this study assuming full constraints between bone and bone, between bone and lag screw, and between bone and distal locking screw. The general contact condition was applied using a friction coefficient of 0.42 to allow for optimal movement.

A total of 24 FEMs were tested using combinations of 8 different fracture levels and 3 different nail types. The stresses around CMNs and cortical bones were investigated with emphasis on the fracture level, nail length, and number of distal locking screws in the FEMs and then compared to the yield strength. The yield strength values of cortical bones and CMNs were referenced from earlier publications (Table 2) [18,19].

Results

Stress distribution on cortical bone

Peak von Mises stress (PVMS) on cortical bones was greatest around the distal locking screw hole in all models and tended to increase with decreasing fracture level.

PVMS on the medial cortex around this site was greater than the yield strength at fracture level $\geq$ 35 mm below the LT in FEMs fixed with type A and B CMNs (Figs. 2 and 3). PVMS on cortical bones was less than the yield strength in all models fixed with type C CMNs (Fig. 4) (Table 3).

Stress distribution on nail body and lag screw

The PVMS site on the nail body tended to move downwards from the junction with the lag screw through the fracture site to the junction with the distal locking screw and the PVMS tended to increase with decreasing fracture level. However, the PVMS at the junction of the nail body and the lag screw in high ST fracture

Table 1
Material properties applied for the FE model analysis.

	Elastic Modulus(E) (MPa)	Poisson's ratio(v)
Cortical bone	17000	0.3
Cancellous bone	920	0.2
Implant (TI6Al4V)	113800	0.342

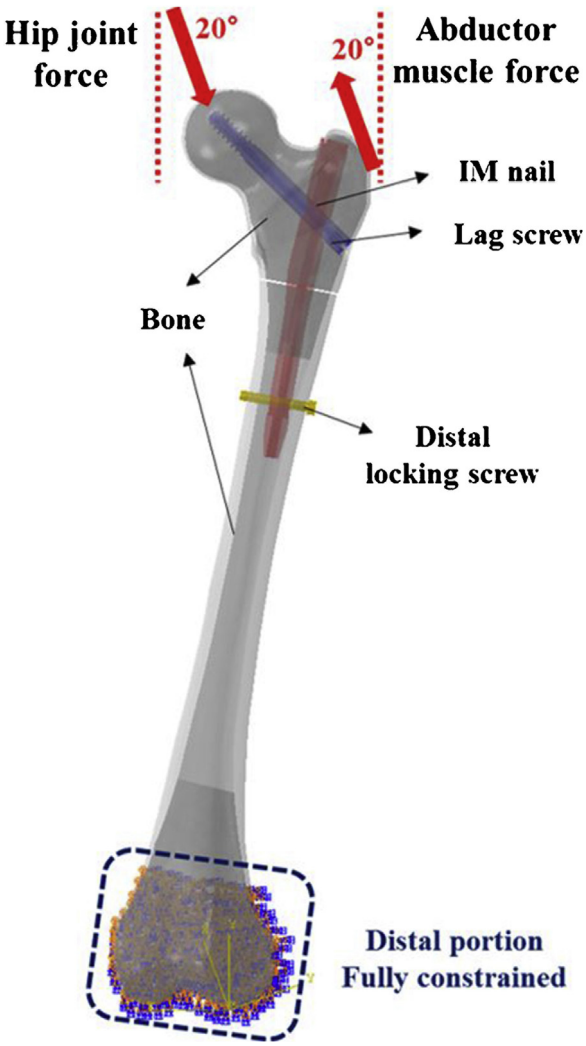

Fig. 1. Loading condition of the analysis model; Hip joint force (F_H), 2058 N (body weight×300%); Abductor muscle force, 686 N (body weight×100%).

Table 2
Yield strength of bone and material.

Region	Yield Strength (MPa)
Cortical bone	107.9
TI6Al4V	880

models just below the LT (0 mm) was greater than the PVMSs in the FEMs at fracture levels ≤ 30 mm below the LT regardless of nail type even though these PVMSs were less than the yield strength.

PVMSs in FEMs fixed with type A CMNs were greater than the yield strength at fracture levels ≥ 35 mm below the LT and were located at the junction of the nail body and the distal locking screw (Fig. 2). However, all FEMs fixed with type B and C CMNs showed PVMSs less than the yield strength on the nail body regardless of the fracture level (Figs. 3 and 4) (Table 3).

PVMS on the lag screw was greatest at the junction with the nail body regardless of the fracture level or nail type. However, all models showed PVMSs less than the yield strength (Table 3).

Stress distribution on distal locking screw

PVMS on the distal locking screw was greatest at the junction with the nail body. At fracture levels ≥ 35 mm below the LT, PVMS in FEMs fixed with type A CMNs were greater than the yield strength on the medial side of the junction with the nail body. However, PVMS on the distal locking screw in all FEMs fixed with type B and type C CMNs was less than the yield strength (Table 3).

Discussion

Stress distribution analysis using FEMs is accepted as a useful method for predicting the biomechanical behavior of orthopedic implants under certain loading conditions [20–23]. This FEA suggested that the use of short CMNs 200 mm in length with 2 distal locking screws is a safe option under the assumptions of anatomical reduction and fracture gap ≤ 1 mm in ST FEMs. However, at fracture levels ≥ 35 mm below the LT, the use of short CMNs 170 mm or 200 mm in length with 1 distal locking screw in these FEMs would increase the risk of fixation failure or peri-implant fracture.

CMNs have been widely used in the surgical management of ST fractures with clinical outcomes superior to those of other extramedullary devices [2–6]. Both short and long CMNs are currently used. Short CMNs are used for high ST fractures while long CMNs are used for low and extended ST fractures [24]. However, there are no clear indications for short CMNs at specific levels of ST fractures. Long CMNs have longer working lengths than short CMNs and are designed, in principle, to provide improved stability. Nevertheless, short CMNs have certain advantages over long CMNs, namely shorter operation and fluoroscopy times, less blood loss and fewer blood transfusions, and lower device cost than long CMNs [8,9]. However, there is a lack of evidence in relevant literature on the appropriate nail length and number of distal locking screws required at the various ST fracture levels. With regards to the bone-implant construct, an earlier study compared the strengths between the different long CMN types used in the surgical management of ST fractures [25]. However, there is little information in published literature on the fixation strengths of short CMNs according to fracture levels in ST fractures and the stresses surrounding them. Therefore, this study compared the strengths of bone-implant constructs at various fracture levels fixed using 3 different short CMN types, and suggested the appropriate fracture levels for their use under the assumptions of anatomical reduction and fracture gap ≤ 1 mm in ST fractures.

All short CMN types used in this study showed similar stress distribution and PVMS location around the cortical bone and nail at corresponding fracture levels. PVMS on the cortical bone around the nail was greatest at the distal locking screw hole irrespective of nail type or fracture level. This finding suggests that the distal locking screw hole at the medial or lateral cortex may be a stress-riser causing peri-implant fracture or fixation failure following ST fracture fixation using a short CMN. As shown in our study, especially when low ST fractures ≥ 35 mm below the LT are fixed using short CMNs 170 mm or 200 mm in length with 1 distal locking screw, the risk increases abruptly because PVMS at the site is greater than the yield strength. The PVMS site on the nail body tended to move downwards from the junction of the nail body and the lag screw through the fracture site to the junction of the nail body and the distal locking screw with decreasing fracture level. This result is consistent with results of earlier studies that reported breakage of the CMN system at 3 principal nail points, namely: the junction of the nail and the lag screw, the distal locking screw, and the fracture site, especially as the lag screw hole and the distal locking screw hole of the nail body are weak points due to the narrow cross-sectional area of the nail [26,27]. PVMSs within the implant were greater than the yield strength at the junction of the nail with distal locking screw and distal locking screw itself when low ST fractures ≥ 35 mm below the LT are fixed with short CMNs 170 mm in length with 1 distal locking screw. In contrast, when a

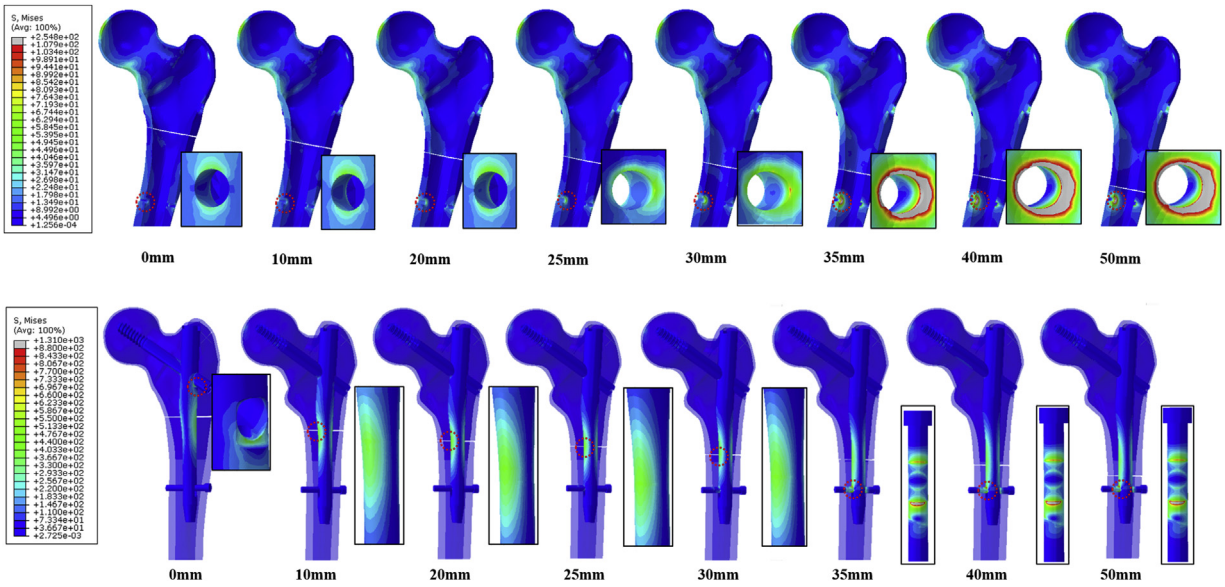

Fig. 2. Stress distribution around the femoral cortical bone (top) and implant (bottom) during type A nail fixation. The enlarged image portion represents the point at which the peak stress was observed.

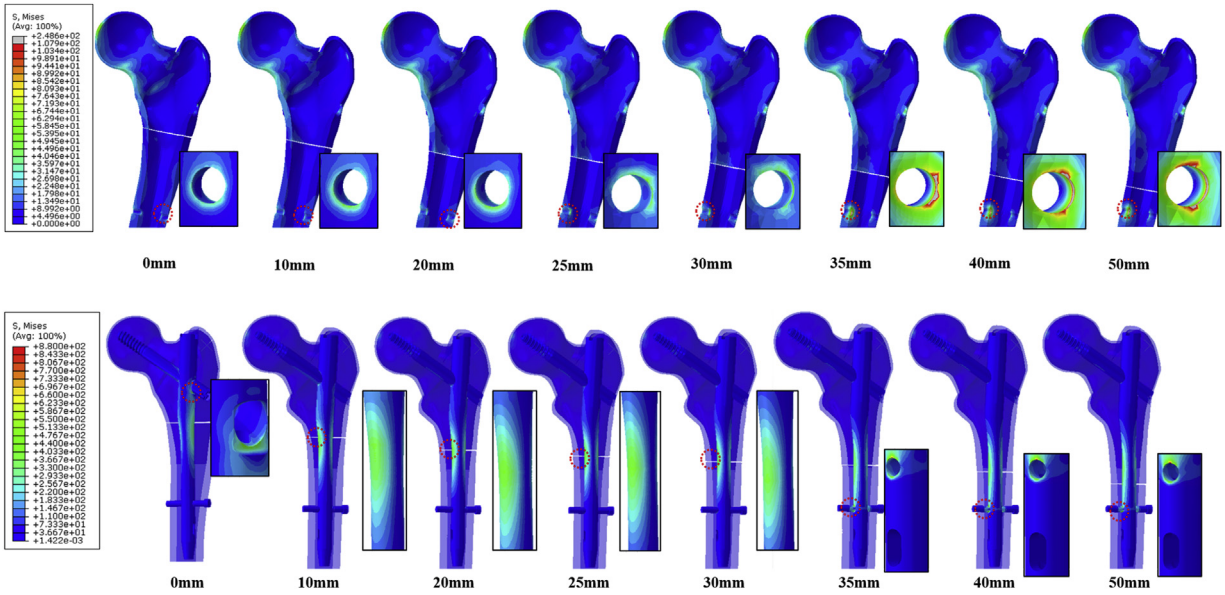

Fig. 3. Stress distribution around the femoral cortical bone (top) and implant (bottom) during type B nail fixation. The enlarged image portion represents the point at which the peak stress was observed.

200 mm CMN with 1 distal locking screw was used, PVMS greater than the yield strength within the implant was not observed. It has been suggested that the short distance from the most distal fracture line to the distal locking screw hole may be a predictor of implant failure at the distal locking screw hole [24]. This would imply that 200 mm nails would be more effective for stress dispersion and stable fixation in ST fractures than 170 mm nails. However, when fixation is performed using short CMNs 200 mm in length with 1 distal locking screw, PVMSs at the 2 sites mentioned above were about 85% of the yield strength. Therefore, we reckon that the use of short CMNs 200 mm in length with 1 distal locking screw is inappropriate for ST fractures $\geq$ 35 mm below the LT due to the risk of nail breakage. In contrast, ST fracture FEMs fixed using short CMNs 200 mm in length with 2 distal locking screws showed PVMSs less than the yield strength both at the cortical bone and within the implant regardless of the fracture level. This may be because distally concentrated stresses are distributed to the junction of the nail with 2 distal locking screws, the 2 distal locking screws themselves, and their cortical screw holes.

Finally, the 3 short CMN types tested in our study can be used in the surgical management of ST fractures $\leq$ 30 mm below the LT under the assumptions of anatomical reduction and fracture gap $\leq$ 1 mm. However, only short CMNs 200 mm in length with 2 distal locking screws can lower the risk of fixation failure in low ST fractures $\geq$ 35 mm below the LT.

Anatomical reduction and the minimal fracture gap are essential for uneventful bony union without the risk of fixation failure in ST fractures. Therefore, this study was performed under the assumptions of anatomical reduction and fracture gap of 1 mm. However, clinical conditions may be different from this

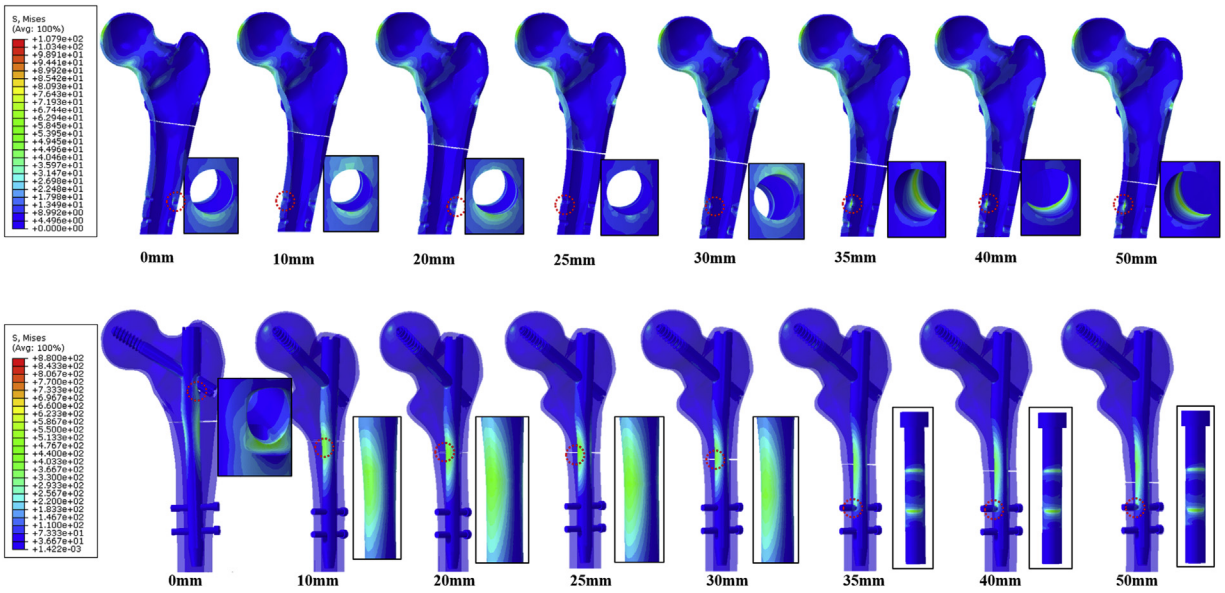

Fig. 4. Stress distribution around the femoral cortical bone (top) and implant (bottom) during type C nail fixation. The enlarged image portion represents the point at which the peak stress was observed.

Table 3
Peak von Mises stress (PVMS) at cortical bone and nail.

Fracture level	Peak Von Mises Stress (MPa)											
	Cortical bone			Nail body			Lag screw			Distal locking screw		
	Type A	Type B	Type C	Type A	Type B	Type C	Type A	Type B	Type C	Type A	Type B	Type C
0mm	48	45	41	472	508	661	247	300	298	140	174	154
10mm	56	53	42	385	387	387	178	223	222	163	215	185
20mm	62	58	45	424	420	420	157	161	161	172	214	202
25mm	72	61	47	422	414	422	243	171	190	217	177	180
30mm	93	77	42	400	391	391	253	159	181	332	179	166
35 mm	**238***	**249***	85	**1250***	780	373	348	154	190	**1310***	742	422
40mm	**262***	**106***	82	**1243***	783	367	299	153	190	**1300***	744	424
50mm	**247***	**202***	88	**1244***	783	367	283	153	190	**1306***	792	422

* Higher than the yield strength (MPa): cortical bone 107.9; implant(Ti6Al4V) 880.

ideal situation. It is therefore necessary to conduct further studies under conditions of non-anatomical reduction or fracture gap > 1 mm to verify the availability and safety of short CMNs in ST fractures.

There are some limitations to this study. First, the complex physiologic force components around the ST area during normal ambulation were simplified. This FEA used only axial loading to simulate the forces of a 1-legged stance. This loading condition was considered appropriate for this FEA because protected partial weight-bearing using walking aids after surgery is clinically allowed until bony union is achieved. Second, we could not determine the exact interaction between the implant and the bone. Although the friction coefficient of 0.42 was taken as the general contact, it is difficult to accept this value for perfect reproducibility as it is hard to know exactly what happens at the interface between the implant and the bone.

A major strength of this study is that, to our knowledge, it is the first FEA to investigate the stress distribution around short CMNs used in the fixation of ST fractures of various levels and evaluate the fixation strength of each short CMN type. Another strength of this study is that it proposes the most appropriate short CMN type for ST fractures at the different fracture levels. Further large multicenter clinical studies are needed to confirm the results of this study and to verify the availability of short CMNs for ST fractures as this is an experimental study using FEA.

Conclusion

Short CMNs 170 mm or 200 mm in length with 1 distal locking screw can be used limitedly in relatively high ST fractures ≤ 30 mm below the LT under the assumptions of anatomical reduction and fracture gap ≤ 1 mm. Short CMNs 200 mm in length with 2 distal locking screws may be considered available treatment options for the fixation of transverse ST fractures under the same assumptions.

Declaration of Competing Interest

There are no conflicts of interest for the authors of the present report.

Source of funding

No external funding was received in support of this study.

Transparency document

The Transparency document associated with this article can be found in the online version.

Acknowledgment

We would like to thank Editage (www.editage.co.kr) for English language editing.

References

[1] Bedi A, Toan Le T. Subtrochanteric femur fractures. Orthop Clin North Am 2004;35:473–83.
[2] Barquet A, Mayora G, Fregeiro J, Lopez L, Rienzi D, Francescoli L. The treatment of subtrochanteric nonunions with the long gamma nail: twenty-six patients with a minimum 2-year follow-up. J Orthop Trauma 2004;18:346–53.
[3] Saarenpaa I, Heikkinen T, Jalovaara P. Treatment of subtrochanteric fractures. A comparison of the Gamma nail and the dynamic hip screw: short-term outcome in 58 patients. Int Orthop 2007;31:65–70.
[4] Hotz TK, Zellweger R, Kach KP. Minimal invasive treatment of proximal femur fractures with the long gamma nail: indication, technique, results. J Trauma 1999;47:942–5.
[5] Kim KK, Won Y, Smith DH, Lee GS, Lee HY. Clinical results of complex subtrochanteric femoral fractures with long cephalomedullary hip nail. Hip Pelvis 2017;29:113–9.
[6] Irgit K, Richard RD, Beebe MJ, Bowen TR, Kubiak E, Horwitz DS. Reverse oblique and transverse intertrochanteric femoral fractures treated with the long cephalomedullary nail. J Orthop Trauma 2015;29:e299–304.
[7] Horwitz DS, Tawari A, Suk M. Nail length in the management of intertrochanteric fracture of the femur. J Am Acad Orthop Surg 2016;24:e50–8.
[8] Okcu G, Ozkayin N, Okta C, Topcu I, Aktuglu K. Which implant is better for treating reverse obliquity fractures of the proximal femur: a standard or long nail? Clin Orthop Relat Res 2013;471:2768–75.
[9] Boone C, Carlberg KN, Koueiter DM, Baker KC, Sadowski J, Wiater PJ, et al. Short versus long intramedullary nails for treatment of intertrochanteric femur fractures (OTA 31-A1 and A2). J Orthop Trauma 2014;28:e96–e100.
[10] Engoren M, Mitchell E, Perring P, Sferra J. The effect of erythrocyte blood transfusions on survival after surgery for hip fracture. J Trauma 2008;65:1411–5.
[11] Kwon GJJM, Oh JK. Lee SJ effects of screw configuration on biomechanical stability during extra-articular complex fracture fixation of the distal femur treated with locking compression plate. J Biomed Eng Res. 2010;31:199–209.
[12] Lee S, Chung CK, Oh SH, Park SB. Correlation between bone mineral density measured by dual-energy X-Ray absorptiometry and hounsfield units measured by diagnostic CT in Lumbar Spine. J Korean Neurosurg Soc 2013;54:384–9.
[13] Rho JY, Hobatho MC, Ashman RB. Relations of mechanical properties to density and CT numbers in human bone. Med Eng Phys 1995;17:347–55.
[14] Morgan EF, Bayraktar HH, Keaveny TM. Trabecular bone modulus-density relationships depend on anatomic site. J Biomech 2003;36:897–904.
[15] Stoffel K, Dieter U, Stachowiak G, Gachter A, Kuster MS. Biomechanical testing of the LCP–how can stability in locked internal fixators be controlled? Injury 2003;34(Suppl 2):B11–9.
[16] Linde F, Hvid I. The effect of constraint on the mechanical behaviour of trabecular bone specimens. J Biomech 1989;22:485–90.
[17] Taylor M. Finite element analysis of the resurfaced femoral head. Proceedings of the Institution of Mechanical Engineers Part H. J Eng Med 2006;220:289–97.
[18] Bayraktar HH, Morgan EF, Niebur GL, Morris GE, Wong EK, Keaveny TM. Comparison of the elastic and yield properties of human femoral trabecular and cortical bone tissue. J Biomech 2004;37:27–35.
[19] Heiney J, Battula S, Njus G, Ruble C, Vrabec G. Biomechanical comparison of three second-generation reconstruction nails in an unstable subtrochanteric femur fracture model. Proceedings of the Institution of Mechanical Engineers Part H. J Eng Med 2008;222:959–66.
[20] Mahaisavariya B, Sitthiseripratip K, Suwanprateeb J. Finite element study of the proximal femur with retained trochanteric gamma nail and after removal of nail. Injury 2006;37:778–85.
[21] Seral B, Garcia JM, Cegonino J, Doblare M, Seral F. Finite element study of intramedullary osteosynthesis in the treatment of trochanteric fractures of the hip: gamma and PFN. Injury 2004;35:130–5.
[22] Sitthiseripratip K, Van Oosterwyck H, Vander Sloten J, Mahaisavariya B, Bohez EL, Suwanprateeb J, et al. Finite element study of trochanteric gamma nail for trochanteric fracture. Med Eng Phys 2003;25:99–106.
[23] Wang CJ, Yettram AL, Yao MS, Procter P. Finite element analysis of a Gamma nail within a fractured femur. Med Eng Phys 1998;20:677–83.
[24] Ongkiehong BF, Leemans R. Proximal femoral nail failure in a subtrochanteric fracture: the importance of fracture to distal locking screw distance. Inj Extra 2007;38:445–50.
[25] Wu X, Yang M, Wu L, Niu W. A biomechanical comparison of two intramedullary implants for subtrochanteric fracture in two healing stages: a finite element analysis. Appl Bionics Biomech 2015;2015:475261.
[26] von Ruden C, Hungerer S, Augat P, Trapp O, Buhren V, Hierholzer C. Breakage of cephalomedullary nailing in operative treatment of trochanteric and subtrochanteric femoral fractures. Arch Orthop Trauma Surg 2015;135:179–85.
[27] Zafiropoulos G, Pratt DJ. Fractured gamma nail. Injury 1994;25:331–6.